Environmental Chemistry Letters (2018) 16:1457–1462
https://doi.org/10.1007/s10311-018-0756-1

ORIGINAL PAPER

Complexation of plasmid DNA and poly(ethylene oxide)/poly(propylene oxide) polymers for safe gene delivery

Hemant Kumar Daima[1,2,3] · Shiv Shankar[1,2,4] · Amanda Anderson[1] · Selvakannan Periasamy[2] · Suresh Bhargava[2] · Vipul Bansal[1]

Received: 1 February 2018 / Accepted: 16 May 2018 / Published online: 25 May 2018

Abstract

Gene delivery is the process of introducing foreign genetic material, such as DNA or RNA, into host cells. Gene therapy utilizes gene delivery to deliver genetic material with the goal of treating a disease or condition in the cell. Actual viral vectors may have side effects, while actual systems using metal nanoparticles for gene delivery are toxic. Therefore, we designed here a biocompatible tri-block copolymer PEO_{20}–PPO_{69}–PEO_{20} as a gene delivery vector [PEO: poly(ethylene oxide); PPO: poly(propylene oxide)]. We studied the conjugation of PEO_{20}–PPO_{69}–PEO_{20} and DNA using various techniques. Results of gel retardation assay along with zeta potential and dynamic light scattering provide evidence of DNA sequestration. Fourier transform infrared spectroscopy and X-ray photoelectron spectroscopy show that the PO_4^{3-} groups of plasmid DNA are primarily involved during nanoconjugate construction. The integrity and functionality of plasmid DNA within the cellular environment is further demonstrated by the expression of green fluorescent protein gene in *Escherichia coli*. Overall, our findings support the use of block copolymers as delivery systems for mammalian and plant cells.

Keywords Environmental toxicity · Physicochemical · Nanoconjugates · Plasmid DNA · Tri-block copolymer · Gene delivery

Introduction

Viral vectors are favored for nucleic acid transport because of small size, protective core, the presence of receptor-specific moieties and membrane fusogenic elements. However, they have potential side effects that limit their applicability as vectors (Check 2002). Conversely, inorganic nanoparticles provide an opportunity for drug, protein and DNA delivery because of their unique properties. However, environmental toxicity, non-degradability and strong association with different cellular components restrict the use of metal nanoparticles (Daima and Navya 2016; Ghosh et al. 2008; Sokolova and Epple 2008). Therefore, organic materials offer better prospects for delivery applications, since enzymes can easily break them down, reducing the likelihood of hostile environmental impact. Moreover, since cellular environment is composed of organic molecules, it is suitable to employ similar kind of materials for payload delivery applications (Duncan et al. 2006; Satchi-Fainaro and Duncan 2006; Hamley 2003; Kwak and Herrmann 2010). However, organic nanostructures have not been fully explored for gene delivery applications, and it

✉ Hemant Kumar Daima
hkdaima@jpr.amity.edu

✉ Shiv Shankar
shivbiotech@gmail.com

✉ Vipul Bansal
vipul.bansal@rmit.edu.au

[1] Ian Potter NanoBioSensing Facility, NanoBiotechnology Research Laboratory (NBRL), School of Science, RMIT University, GPO Box 2476 V, Melbourne, VIC 3001, Australia

[2] Centre for Advanced Materials and Industrial Chemistry, School of Science, RMIT University, GPO Box 2476 V, Melbourne, VIC 3001, Australia

[3] Amity University Science and Instrumentation Center-II (AUSIC-II), Amity Institute of Biotechnology, Amity University Rajasthan, Kant Kalwar, NH-11C, Jaipur Delhi Highway, Jaipur, Rajasthan 303002, India

[4] Department of Food Engineering and Bionanocomposite Research Institute, Mokpo National University, Muangun 534-729, South Korea

is important to develop new efficient organic materials in order to realize their full potential and to overcome the safety issues.

In this spirit, polyplexes have been designed through entropically driven interactions of DNA and synthetic polymers. Polyplexes can be formed through electrostatic interactions between negatively charged DNA and positively charged groups of polymers (Boussif et al. 1995; Gebhart and Kabanov 2003; Pack et al. 2005). However, the use of cationic polymers in such polyplexes has been noted to strongly condense DNA, which reduces the payload delivery efficiency along with enhanced cytotoxicity (Wong et al. 2007). Therefore, amphiphilic block copolymers have also been screened to enhance DNA vaccination for therapeutic needs as biologically active block copolymers can self-assemble into micellar structures and have spontaneous associations with DNA (Gebhart and Kabanov 2003; McIlroy et al. 2009; Torchilin 2007).

In the present study, a biocompatible tri-block copolymer of poly(ethylene oxide)–poly(propylene oxide)–poly(ethylene oxide) [PEO_{20}–PPO_{69}–PEO_{20}] is chosen as a plasmid DNA delivery vector. To understand the interactions between plasmid DNA and PEO_{20}–PPO_{69}–PEO_{20}, a number of sensitive techniques were utilized to establish that PEO_{20}–PPO_{69}–PEO_{20} is proficient in constructing compact nanoconjugates with plasmid DNA.

Experimental

Plasmid DNA isolation, purification and construction of nanoconjugates

Plasmid DNA containing green fluorescent protein (GFP) and ampicillin resistance genes was isolated and purified according to *Shambrook and Russell* with some modifications (Sambrook and Russell 2000). Under vigorous stirring, in 100 mL deionized MilliQ water at 50 °C, 10 g of PEO_{20}–PPO_{69}–PEO_{20} was dissolved to obtain a stock solution. Different volumes of this solution were incubated with a fixed amount of 10 µg plasmid DNA for 2 h at 37 °C to form nanoconjugates.

Preparation of competent cells

Modified $CaCl_2$.$MgCl_2$ method in the presence of tetracycline was employed to make competent cells of *Escherichia coli* DH5α (Sambrook and Russell 2000; Tu et al. 2005). Competent cells were suspended in ice-cold fresh 100 mM $CaCl_2$ solution.

Transformation and gene expression

For transformation, nanoconjugates were mixed with 200 µL of freshly prepared competent cells and incubated on ice. After 30 min, heat shock was given for 90 s at 42 °C, and instantly transferred on ice for 2 min, followed by addition of 800 µL of Luria–Bertani (LB) broth. Finally, cells were incubated at 37 °C for 1 h, followed by spreading 100 µL aliquots on nutrient agar plates containing 10 µg/mL ampicillin. Colonies grown after overnight incubation were counted. 200 µL of competent cells and 800 µL of Luria–Bertani broth were used as negative control, while an equal amount of plasmid DNA under similar conditions was used as a positive control.

Physicochemical characterization

The Fourier transform infrared spectroscopy (FTIR) spectra were recorded in diffused reflectance (DRS) mode using Perkin-Elmer D100 spectrophotometer with a resolution of 4 cm^{-1}. The X-ray photoelectron spectroscopy analyses were performed on THERMO K-Alpha XPS machine, at a pressure better than 1×10^{-9} Torr. The core-level spectra for all the samples were recorded with un-monochromatized Mg Kα radiation (photon energy of 1253.6 eV) at pass energy of 50 eV, electron takeoff angle of 90° and overall resolution at 0.1 eV. All the X-ray photoelectron spectroscopic spectra were background-corrected using Shirley algorithm, and their core-level binding energies were aligned with respect to the adventitious C1s binding energy (BE) of 285 eV (Shirley 1972). Zeta (ζ) potential measurements were taken using Malvern 2000 Zetasizer.

Results and discussion

PEO_{20}–PPO_{69}–PEO_{20} has linear A–B–A architecture, wherein end of one segment is covalently joined to the head of the other segment. In PEO_{20}–PPO_{69}–PEO_{20}, the PPO chain (hydrophobic) has potential to invade lipid bilayers, whereas PEO chain (hydrophilic) weakly adsorbs at the membrane surface. Thus, depending upon the length of PPO/PEO chains, the PEO–PPO–PEO copolymer can act either as a membrane sealant or as a permeabilizer. Furthermore, PEO can offer solubility and cover DNA–copolymer complex from immune recognition, which can protect DNA from degradation (Batrakova and Kabanov 2008; Gebhart and Kabanov 2003; Wang et al. 2012). However, the physicochemical aspects that govern the association of negatively charged plasmid DNA with PEO_{20}–PPO_{69}–PEO_{20} are not well understood; therefore,

we have employed a number of sensitive techniques to understand these interactions.

The DNA compaction ability of PEO_{20}–PPO_{69}–PEO_{20} was evaluated by gel retardation assay using agarose gel electrophoresis, wherein an equal amount of DNA was loaded in each well (Fig. 1A). The increasing amounts of PEO_{20}–PPO_{69}–PEO_{20} with respect to plasmid DNA (lanes 2–8) led to increasing retardation of plasmid DNA mobility, since an increasing amount of plasmid DNA retained in the wells. In order to further understand this mechanism, samples were subjected to zeta potential measurements, which revealed a continuous reduction in negative zeta value of plasmid DNA from − 30.6 to − 10.8 mV with an increase in DNA-to-polymer ratio of 1:100 (Fig. 1B). Since PEO_{20}–PPO_{69}–PEO_{20} is a non-ionic polymer, the shift in the zeta potential value from highly negative toward neutral is indicative of increasing DNA sequestration, potentially through H-bonding interactions between the DNA and the polymer. The zeta potential measurements support the observations from gel migration assay, which suggested a reduction in DNA mobility, potentially due to a reduction in overall negative charge as a function of the increase in polymer concentration. Figure 1C shows a change in hydrodynamic diameter of plasmid DNA/PEO_{20}–PPO_{69}–PEO_{20} nanoconjugates. Interestingly, an increase in polymer concentration with respect to plasmid DNA led to dramatic reduction in diameter. This suggests that as the concentration of polymer is increased, either the number of micelles is increased at the cost of particle size, or due to the presence of larger amount of polymer, the micelles become more compact.

As demonstrated in Fig. 2 (Panel-1) pure plasmid DNA displays characteristic vibrational frequencies of DNA in the 1700–1500 cm^{-1} region and phosphate (PO_4^{3-}) stretching frequencies in 1250–1050 cm^{-1} (curve 2). Two strong absorption bands at 1230 and 1088 cm^{-1} (marked*) are assigned to asymmetric and symmetric stretching vibrations of PO_4^{3-} group, respectively. Vibrational frequencies at 1701, 1661, 1610, 1582 (shoulder), 1534 and 1482 cm^{-1} are assigned to guanine (C_7=N stretching), thymine (C_2=O stretching), adenine (C_7=N stretching), purine stretching (N_7), in-plane vibration of cytosine and guanine and in-plane vibration of cytosine, respectively. Additionally, C–C deoxyribose stretching was observed at 969 cm^{-1}, while deoxyribose B-marker frequency was observed at 875 cm^{-1}. The detected plasmid DNA frequencies are in agreement with the published literature (Choosakoonkriang et al. 2003; Taillandier and Liquier 1992). Comparative analysis of spectra provided evidence for interaction between the PO_4^{3-} groups of plasmid DNA and PEO_{20}–PPO_{69}–PEO_{20}. In pristine PEO_{20}–PPO_{69}–PEO_{20} (curve 1), there were no vibrational frequencies between 1700 and 1500 cm^{-1} region, but the signatures appeared in the nanoconjugates without any significant changes (curves 3 and 4). As displayed in curves 3 and 4 (plasmid DNA/polymer, 1:1 and 1:10, respectively), after interaction, shifts in vibrational frequencies were observed in both the asymmetric and symmetric stretching of PO_4^{3-} from 1230 to 1237 (1:1) and 1242 (1:10) cm^{-1}, and from 1088 to 1118 cm^{-1}, respectively. However, there were no considerable changes in other functional groups; thus, Fourier transform infrared spectroscopy provided strong confirmation that PO_4^{3-} of plasmid DNA interacts with PEO_{20}–PPO_{69}–PEO_{20} during nanoconjugates formation.

As illustrated in Fig. 2 (Panel-2A), core-level X-ray photoelectron spectroscopy spectra of C1*s* recorded for plasmid DNA can be deconvoluted into three energy levels. Binding energies (BE) maxima at 285.0, 286.4 and 287.9 eV can be assigned to the aromatic carbon chain, carbon attached to O and N species, and C=O present in nitrogenous bases,

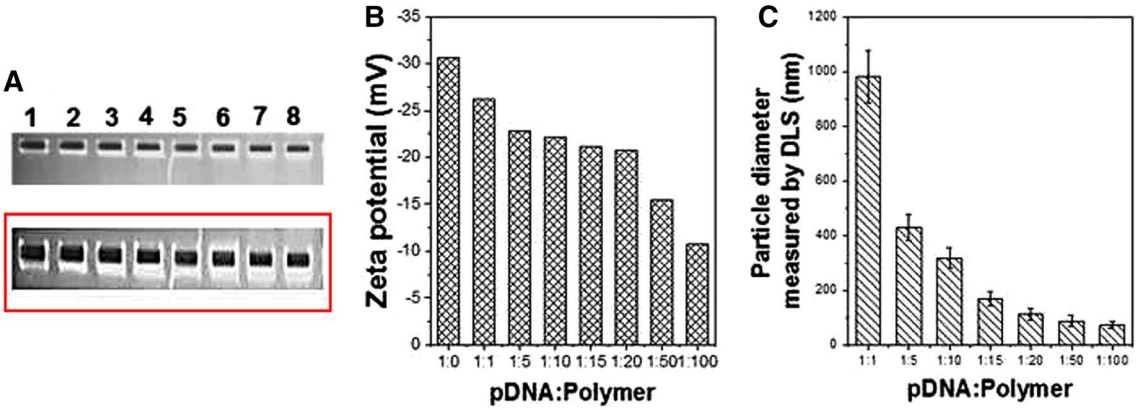

Fig. 1 **A** Gel retardation assay showing plasmid DNA compaction ability of PEO_{20}–PPO_{69}–PEO_{20}, wherein lane 1 corresponds to plasmid DNA; lanes 2–8 correspond to plasmid DNA/polymer nanoconjugates of 1:1, 1:5, 1:10, 1:15, 1:20, 1:50 and 1:100 ratios. The bottom panel shows the vertically elongated and 50% sharpen view of the wells for clarity. **B** Zeta potential measurements, and **C** hydrodynamic diameter of plasmid DNA/PEO_{20}–PPO_{69}–PEO_{20} nanoconjugates of different ratios. PEO: poly(ethylene oxide); PPO: poly(propylene oxide)

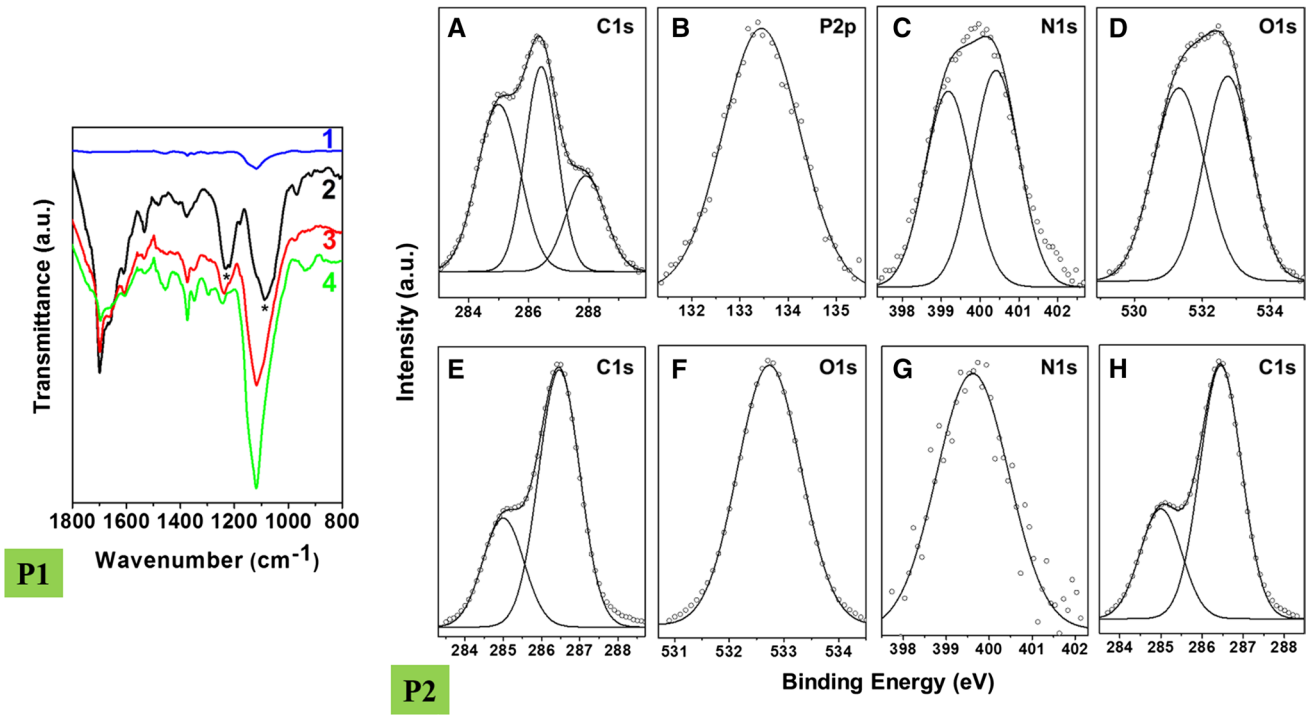

Fig. 2 Panel-1 displays Fourier transform infrared spectroscopic (FTIR) spectra of PEO_{20}–PPO_{69}–PEO_{20} (curve 1), plasmid DNA (curve 2), and after nanoconjugation (curves 3 and 4), confirming involvement of PO_4^{3-} group of plasmid DNA in the interaction during the nanoconjugates construction. Panel-2 illustrates the core-level X-ray photoelectron spectra (XPS) of principal elements present in plasmid DNA (**A**–**D**); C1*s* and O1*s* present in PEO–PPO–PEO (**E** and **F**); N1*s* in 1:1 ratio plasmid DNA:PEO_{20}–PPO_{69}–PEO_{20} (**G**); and C1*s* in 1:10 ratio plasmid DNA:PEO_{20}–PPO_{69}–PEO_{20} (**H**). PEO: poly(ethylene oxide); PPO: poly(propylene oxide)

correspondingly. The core-level X-ray photoelectron spectroscopy spectrum of P2p (Fig. 2, Panel-2B) arising from plasmid DNA shows binding energy maximum at 133.4 eV, and it can be specified to PO_4^{3-} groups of plasmid DNA. Figure 2, Panel-2C, shows X-ray photoelectron spectroscopy spectrum of N1*s* core level in plasmid DNA, which can be deconvoluted into two energy levels, in which the lower binding energy component at 399.2 eV can be assigned to the –C=N group, whereas the higher binding energy feature at 400.4 eV can be devoted to $–NH_2$. Similarly, the O1*s* recorded for plasmid DNA can be disintegrated into two energy levels at 531.3 and 532.75 eV maxima, which can be allotted to phosphate-oxygen and deoxyribose sugar-oxygen, respectively. Further demonstrated in Fig. 2 (Panel-2E–F) are X-ray photoelectron spectroscopy spectra of C1*s* and O1*s* present in PEO_{20}–PPO_{69}–PEO_{20}. The core-level C1*s* spectrum can be deconvoluted into two major energy levels. The lower binding energy at 285.0 eV is assigned to alkyl chain of PEO_{20}–PPO_{69}–PEO_{20}, and the higher binding energy at 286.5 eV can be assigned to carbon attached to oxygen. Binding energy at 532.7 eV was observed for O1*s* core-level spectrum originating from PEO_{20}–PPO_{69}–PEO_{20}. Since pristine PEO_{20}–PPO_{69}–PEO_{20} does not have nitrogen, N signatures were not detected. Nevertheless, N signatures appeared in plasmid DNA and polymer nanoconjugates, further confirming their association. Representative core-level X-ray photoelectron spectroscopy spectra of N1s (in plasmid DNA:PEO-PPO-PEO at 1:1 ratio) are illustrated in Fig. 2 (Panel-2G), which shows a single binding energy component at 399.6 eV. Furthermore, core-level X-ray photoelectron spectroscopy spectra of C1*s* (at 1:10 ratio) are presented in Fig. 2 (Panel-2H). It was interesting to observe that there were no significant changes in the binding energies of C1*s*, even after conjugation at different weight ratios. The C1*s* X-ray photoelectron spectroscopy spectrum recorded for plasmid DNA:PEO–PPO–PEO (1:10 ratio) can be deconvoluted into two energy levels. The lower binding energy is observed at 285.0 eV, and the higher binding energy is recorded at 286.5 eV, which are comparable to PEO_{20}–PPO_{69}–PEO_{20}.

Coexisting N and P are indicators of DNA since their presence is typically unaffected by surface contaminations. Still, in DNA nucleotides, N atoms are present in higher amount than P, and N has a higher X-ray photoelectron spectroscopy cross section. Therefore, between P and N, N can provide a more reliable reference for composition measurements (Petrovykh et al. 2003). Based on X-ray photoelectron spectroscopy analysis as represented in Table 1, it is

Table 1 Atomic percentage of oxygen, carbon and nitrogen in plasmid DNA, PEO_{20}–PPO_{69}–PEO_{20} and their nanoconjugates. PEO: poly(ethylene oxide); PPO: poly(propylene oxide)

Sample	O atomic%	C atomic%	N atomic%	C/N ratio
PEO–PPO–PEO (P)	12.72	37.28	–	–
DNA (D)	12.12	33.51	4.38	7.65
D/P 1:1	12.77	36.04	1.16	31.07
D/P 1:5	12.16	37.05	0.78	47.50
D/P 1:10	12.45	37.02	0.53	69.85

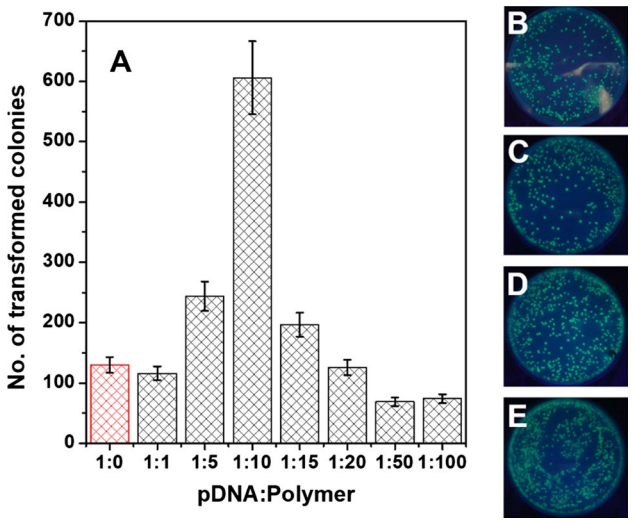

Fig. 3 **A** Number of transformed colonies grown on ampicillin plates (10 μg/mL) for varying ratios of plasmid DNA and PEO_{20}–PPO_{69}–PEO_{20}. **B**–**E** Images of transformed colonies showing integrity and expression of green fluorescent protein (GFP) gene. Plasmid DNA (**B**), plasmid DNA:PEO_{20}–PPO_{69}–PEO_{20} (**C**–**E**) at 1:1 (**C**), 1:5 (**D**) and 1:10 (**E**) ratios, respectively. PEO: poly(ethylene oxide); PPO: poly(propylene oxide)

noteworthy that in nanoconjugates, with the increasing concentration of polymer (with respect to plasmid DNA), C/N ratio increased significantly. The constant increase in C/N ratio indicates that the plasmid DNA is efficiently encapsulated in nanoconjugates.

Once the chemical interactions were confirmed, the nanoconjugates were tested for their proof-of-concept applicability in bacterial gene transformation. Ampicillin was used for the selection of transformation-positive bacteria during transformation because *Escherichia coli* DH5α originally did not has an ampicillin-resistant gene; therefore, only those cells that had taken up the foreign plasmid DNA (containing an ampicillin-resistant gene) could survive on the antibiotic containing plates. It is notable that only a few competent bacterial cells were able to uptake freely available plasmid DNA (without PEO_{20}–PPO_{69}–PEO_{20}) as some bacterial colonies were grown on antibiotic containing plates (positive control at 1:0 ratio (Fig. 3A). Conversely, competent bacterial cells themselves could not survive on ampicillin plates due to the lack of the resistant gene and no colonies were developed in the negative control.

Transformation with nanoconjugates revealed that with the increasing ratio of PEO_{20}–PPO_{69}–PEO_{20} (with respect to plasmid DNA), the number of transformed colonies exhibited steep rise up to 1:10 weight ratios and reached the maximum. Further increment in the polymer concentration showed a significant decline till the evaluated ratios. Therefore, at 1:10 ratio transformation was maximum, and in comparison with pure plasmid DNA, it showed over sixfold higher transformation. Besides, gene expression is also a vital phenomenon by which information from a gene can be utilized to synthesize a functional product and it is essential to protect DNA from degradation during delivery. Therefore, the capability of transformed plasmid DNA to retain its functional integrity, i.e., it can synthesize gene product, is also demonstrated in cellular environment. After transformation, if plasmid DNA is delivered into cells and stays functional, green fluorescent protein (GFP) will be synthesized in the cells through the expression of gene. Figure 3B–E exhibits fluorescence originating from transformed bacterial colonies through the expression of green fluorescent protein gene, thus confirming the integrity and functionality of plasmid DNA in the cellular environment.

Conclusion

The present work provides insights into the physicochemical aspects that direct a PEO_{20}–PPO_{69}–PEO_{20} block copolymer to formulate nanoconjugates with plasmid DNA. Detailed analysis of these nanoconjugates revealed that the PO_4^{3-} group of plasmid DNA is primarily involved in the interaction with the block copolymer. The size of nanoconjugates depends on the concentration of PEO_{20}–PPO_{69}–PEO_{20} with respect to plasmid DNA. Further, it is established that in the presence of PEO_{20}–PPO_{69}–PEO_{20}, the plasmid DNA condenses and it can be efficiently transported inside the cells. Moreover, it was confirmed by the expression of genes within the cellular environment that the integrity and functionality of plasmid DNA was preserved in nanoconjugates. The vast molecular diversity of block copolymers offers new opportunities in fine-tuning their physicochemical properties to obtain nanoconjugates for a variety of applications with reduced toxicity.

Acknowledgements HKD gratefully acknowledges Government of India for National Overseas Scholarship and Japan Science and Technology (JST) Agency, Japan, for Sakura Science Asia Youth Exchange Fellowship. SS gratefully acknowledges Australian Government for an Endeavour Postdoctoral Research Award. VB acknowledges the Australian Research Council for a Future Fellowship (FT140101285) and

Ian Potter Foundation for establishing Sir Ian Potter NanoBioSensing Facility at RMIT University. Authors acknowledge the support of RMIT node of AMMRF for providing technical assistance and access to characterization facilities.

References

Batrakova EV, Kabanov AV (2008) Pluronic block copolymers: evolution of drug delivery concept from inert nanocarriers to biological response modifiers. J Control Release 130:98–106. https://doi.org/10.1016/j.jconrel.2008.04.013

Boussif O, LezoualC'H F, Zanta MA, Mergny MD, Scherman D, Demeneix B, Behr JP (1995) A versatile vector for gene and oligonucleotide transfer into cells in culture and in vivo: polyethylenimine. Proc Natl Acad Sci USA 92:7297–7301. https://doi.org/10.1073/pnas.92.16.7297

Check E (2002) Gene therapy: a tragic setback. Nature 420:116–118. https://doi.org/10.1038/420116a

Choosakoonkriang S, Lobo BA, Koe GS, Koe JG, Middaugh CR (2003) Biophysical characterization of PEI/DNA complexes. J Pharm Sci 92:1710–1722. https://doi.org/10.1002/jps.10437

Daima HK, Navya PN (2016) Rational engineering of physicochemical properties of nanomaterials for biomedical applications with nanotoxicological perspectives. Nano Converg 3:1–14. https://doi.org/10.1186/s40580-016-0064-z

Duncan R, Ringsdorf H, Satchi-Fainaro R (2006) Polymer therapeutics: polymers as drugs, drug and protein conjugates and gene delivery systems: past, present and future opportunities. J Drug Target 14(6):337–341. https://doi.org/10.1080/10611860600833856

Gebhart CL, Kabanov AV (2003) Perspectives on polymeric gene delivery. J Bioact Compat Polym 18:147–166. https://doi.org/10.1177/0883911503018002005

Ghosh P, Han G, De M, Kim CK, Rotello VM (2008) Gold nanoparticles in delivery applications. Adv Drug Deliv Rev 60:1307–1315. https://doi.org/10.1016/j.addr.2008.03.016

Hamley IW (2003) Nanotechnology with soft materials. Angew Chem Int Ed 42:1692–1712. https://doi.org/10.1002/anie.200200546

Kwak M, Herrmann A (2010) Nucleic acid/organic polymer hybrid materials: synthesis, superstructures, and applications. Angew Chem Int Ed 49:8574–8587. https://doi.org/10.1002/anie.200906820

McIlroy D, Barteau B, Cany J, Richard P, Gourden C, Conchon S, Pitard B (2009) DNA/amphiphilic block copolymer nanospheres promote low-dose DNA vaccination. Mol Ther 17:1473–1481. https://doi.org/10.1038/mt.2009.84

Pack DW, Hoffman AS, Pun S, Stayton PS (2005) Design and development of polymers for gene delivery. Nat Rev Drug Discov 4:581–593. https://doi.org/10.1038/nrd1775

Petrovykh DY, Kimura-Suda H, Whitman LJ, Tarlov MJ (2003) Quantitative analysis and characterization of DNA immobilized on gold. J Am Chem Soc 125:5219–5226. https://doi.org/10.1021/ja029450c

Sambrook J, Russell D (2000) Molecular cloning: a laboratory manual, 3rd Revised edn. Cold Spring Harbor Laboratory Press, New York. ISBN 978-0879695767

Satchi-Fainaro R, Duncan R (eds) (2006) Polymer therapeutics I: polymers as drugs, conjugates and gene delivery systems. Springer, Berlin, pp 1–8. ISBN 978-3-540-32945-9

Shirley DA (1972) High-resolution X-ray photoemission spectrum of the valence bands of gold. Phys Rev B 5:4709–4714. https://doi.org/10.1103/PhysRevB.5.4709

Sokolova V, Epple M (2008) Inorganic nanoparticles as carriers of nucleic acids into cells. Angew Chem Int Ed 47:1382–1395. https://doi.org/10.1002/anie.200703039

Taillandier E, Liquier J (1992) Infrared spectroscopy of DNA. Methods Enzymol 211:307–335. https://doi.org/10.1016/0076-6879(92)11018-E

Torchilin V (2007) Micellar nanocarriers: pharmaceutical perspectives. Pharm Res 24:1–16. https://doi.org/10.1007/s11095-006-9132-0

Tu Z, He G, Li KX, Chen MJ, Chang J, Chen L, Yao Q, Liu DP, Ye H, Shi J, Xuqian W (2005) An improved system for competent cell preparation and high efficiency plasmid transformation using different *Escherichia coli* strains. Electron J Biotechnol 8:815. https://doi.org/10.2225/vol8-issue1-fulltext-8

Wang J-Y, Marks J, Lee KYC (2012) Nature of interactions between PEO–PPO–PEO triblock copolymers and lipid membranes: (I) effect of polymer hydrophobicity on its ability to protect liposomes from peroxidation. Biomacromolecules 13:2616–2623. https://doi.org/10.1021/bm300847x

Wong SY, Pelet JM, Putnam D (2007) Polymer systems for gene delivery—past, present, and future. Prog Polym Sci 32:799–837. https://doi.org/10.1016/j.progpolymsci.2007.05.007